



Distribution of glycerol dialkyl glycerol tetraethers in soils from two environmental transects in the USA

Sitindra S. Dirghangi^{a,*}, Mark Pagani^a, Michael T. Hren^b, Brett J. Tipple^c

^a Department of Geology and Geophysics, Yale University, New Haven, CT 06511, USA

^b Center for Integrative Geosciences, University of Connecticut, Storrs, CT 06269, USA

^c Department of Biology, University of Utah, Salt Lake City, UT 84105, USA

ARTICLE INFO

Article history:

Received 17 September 2012

Received in revised form 19 March 2013

Accepted 21 March 2013

Available online 30 March 2013

ABSTRACT

Glycerol dialkyl glycerol tetraethers (GDGTs) of both archaeal and bacterial origin form the basis of new temperature proxies applicable to soil, and lake and marine sediments. In soil, branched GDGTs are prevalent and their abundance of methyl or cyclic groups has been calibrated to mean annual temperature (MAT) using MBT and CBT indices. However, soil pH is also known to be an important variable controlling the distribution of branched GDGTs. Precipitation amount helps control soil moisture, as well as pH, and soil moisture is a leading variable affecting microbial diversity and activity in soil. We have evaluated the distribution of GDGTs from two soil transects in the USA: a dry, western transect covering six western states and a wet, east coast transect from Maine to Georgia in order to assess the effect of precipitation on the distribution of soil GDGTs. Our results show distinctly different GDGT distributions across climatic regions, with dry western soils characterized predominantly by thaumarchaeotal isoprenoid (iso) GDGTs and as a consequence, low BIT index values (0.2–0.6) and moist-temperate, east coast transect soils expressing mostly branched (br) GDGTs and higher BIT values (0.9–1). The predominance of iso GDGTs in the western soils is related to the degree of aeration, which in turn is related to precipitation amount, and also to soil pH. We also observed a substantial increase in the offset between measured MAT and MBT/CBT-based MAT below an annual precipitation of 700–800 mm yr⁻¹, implying an impact of precipitation amount on MBT/CBT-based temperature reconstruction. The data suggest that, while soil tetraethers work well as a temperature proxy in moist-temperate regimes, they do not produce reliable measurements of temperature in sediments sourced from areas with < 700–800 mm yr⁻¹ precipitation. Moreover, erosion of soils with low BIT values into lacustrine or marginal marine environments will not be detected via the BIT index, which can potentially affect paleotemperature reconstruction from sediments, and so provide erroneous estimates of soil carbon delivery. BIT index values also show a correlation with precipitation amount. The abundance of iso GDGTs in western transect soils allowed calculation of TEX₈₆ values, but no correlation was found between TEX₈₆ calculated temperature and mean annual temperature.

© 2013 Elsevier Ltd. All rights reserved.

1. Introduction

Reconstruction of ancient ocean and terrestrial temperature values is a fundamental aspect of paleoclimate research and several methodologies based on inorganic proxies (Epstein et al., 1953; Shackleton, 1967; Kennett and Shackleton, 1975; Wefer and Berger, 1991; Nürnberg et al., 1995; Rosenthal et al., 1997; Podlaha et al., 1998; Lear et al., 2000, 2002; Ghosh et al., 2006, 2007; Affek et al., 2008; Mutterlose et al., 2010) and organic proxies (Prah and Wakeham, 1987; Prah et al., 1988; Müller et al., 1998; Liu and Herbert, 2004; Conte et al., 2006; Herbert et al., 2010) have been established. In particular, proxies founded on

the distribution of glycerol dialkyl glycerol tetraethers (GDGTs; Schouten et al., 2002; Wuchter et al., 2004, 2005; Weijers et al., 2006a) are being increasingly used for reconstructing ancient marine and terrestrial temperatures, given their ubiquitous occurrence in ocean and lake sediments and soils (Powers et al., 2004; Pagani et al., 2006; Sluijs et al., 2006; Weijers et al., 2007a,b; Schouten et al., 2008; Liu et al., 2009). Two types of GDGTs are found in natural environments: those of archaeal origin, consisting of isoprenoid (iso) chains, occur mainly in marine and lake environments (Schouten et al., 2000, 2007; Powers et al., 2004) and those of bacterial origin, consisting of branched (br) alkyl chains, occur predominantly in soils (Weijers et al., 2004, 2006a, 2007c).

Soils are characterized by a dominance of br GDGTs (Weijers et al., 2004, 2006a, 2007c), which were first observed in peat bogs (Weijers et al., 2006b), and consist of a group of nine compounds (VIIa,b,c, VIIIa,b,c and IXa,b,c; Fig. 1) with varying numbers of alkyl

* Corresponding author. Tel.: +1 203 606 1268.

E-mail address: sitindra.dirghangi@yale.edu (S.S. Dirghangi).

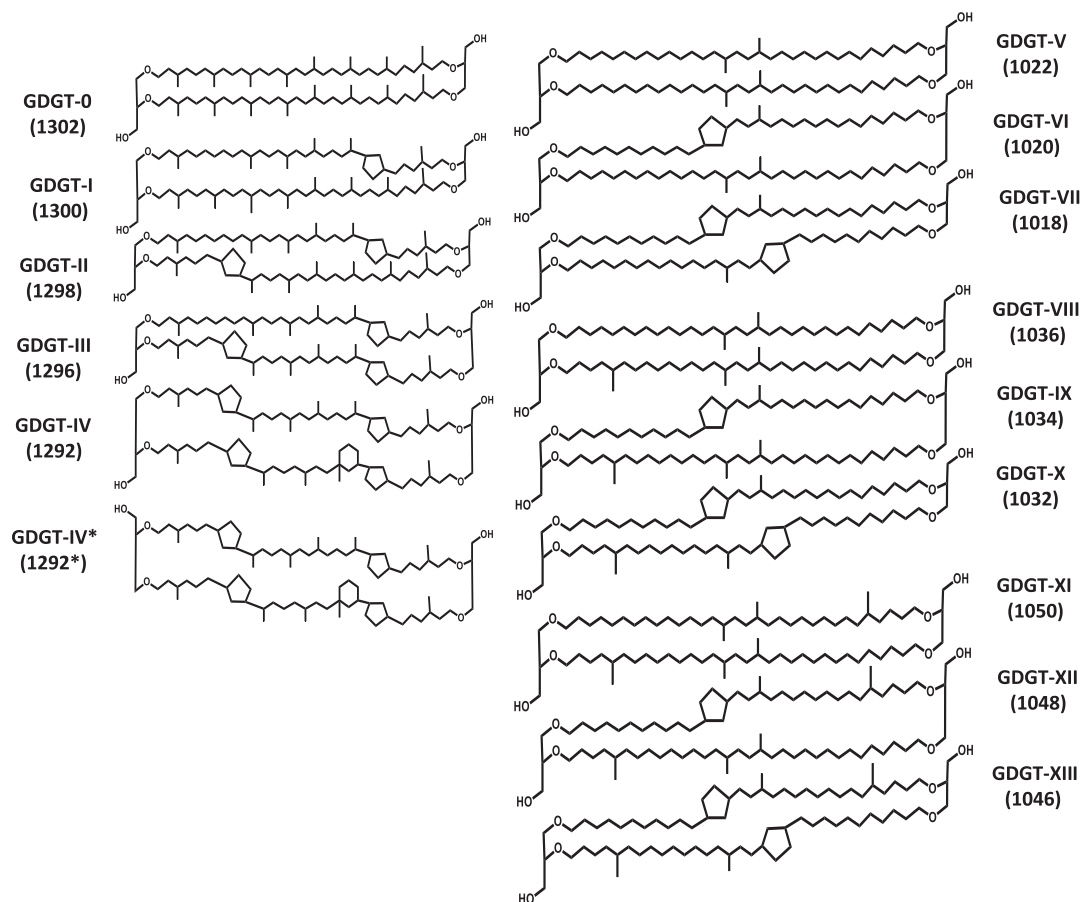


Fig. 1. Structures of GDGTs in soils and sediments; GDGT-0 to GDGT-IV and GDGT-IV* (crenarchaeol regioisomer) are the isoprenoid GDGTs of thaumarchaeal origin, and GDGT-V to GDGT-XIII are the branched GDGTs of bacterial origin.

branches and cyclopentanyl rings and synthesized by facultative anaerobic heterotrophic bacteria, probably belonging to the phylum acidobacteria (Hopmans et al., 2004; Weijers et al., 2004, 2006b, 2010). Stereochemical studies and carbon isotope measurements indicate a bacterial and heterotrophic origin, respectively (Weijers et al., 2006b, 2010; Oppermann et al., 2010). The $\delta^{13}\text{C}$ values of alkyl moieties released from GDGTs V–XIII by ether cleavage were very similar to (generally depleted by $< 1\%$) $\delta^{13}\text{C}$ values of total organic carbon (TOC; Pancost and Sinninghe Damsté, 2003; Weijers et al., 2010). This observation is consistent with the br GDGT-producing acidobacteria utilizing, as substrate, components of TOC, namely carbohydrates and proteins that are more ^{13}C enriched (Weijers et al., 2010). Further, two strains of acidobacteria have been observed to produce a br GDGT in culture experiments (Sinninghe Damsté et al., 2011). Two indices based on the distribution of br GDGTs have been established (Weijers et al., 2007c): MBT (methylation index of br tetraethers) and CBT (cyclisation ratio of br tetraethers). Methylation of br GDGTs appears to be dominantly controlled by mean annual air temperature (MAT) and soil pH, and the cyclisation of br GDGTs is controlled mainly by pH (Weijers et al., 2007c). MAT can thus be estimated using both MBT and CBT (Weijers et al., 2007c) and both have been utilized to infer variations in temperature and environmental conditions during various time periods in the past (Weijers et al., 2007a,b; Donders et al., 2009; Rueda et al., 2009; Hren et al., 2010). Br GDGTs are introduced from soils to shallow marine and lacustrine environments via erosion, although recent evidence indicates an additional in situ aquatic, rather than soil, provenance in lacustrine environments (Tierney and Russell, 2009). However, apart from

br GDGTs, some iso GDGTs of thaumarchaeotal origin are also observed in soils, generally in small amount, as evident from BIT or br isoprenoid tetraether index values in soils that are generally < 0.99 with an average value of 0.90 (Schouten et al., 2013 and references therein, e.g. Weijers et al., 2006a; Sinninghe Damsté et al., 2008, 2009; Peterse et al., 2009; Huguet et al., 2010; Kim et al., 2010b; Loomis et al., 2011). This is due to the ubiquitous occurrence of thaumarchaeota in soils (Leininger et al., 2006).

Iso GDGTs are the dominant ones in marine environments (Schouten et al., 2002, 2007; Wuchter et al., 2004, 2005) and are abundant in lacustrine environments (Powers et al., 2004). They derive from archaea and comprise a group of six tetraethers with 86 carbons (Fig. 1). Given the available information, GDGT-0 or caldarchaeol (I) is produced predominantly by methanogenic euryarchaea; GDGT-1, -2, and -3 (II–IV) are synthesized by both thermophilic and mesophilic crenarchaea, which have recently been proposed to belong to the phylum Thaumarchaeota (Spang et al., 2010; Pester et al., 2011) and methanotrophic euryarchaea (Schouten et al., 2000; Zhang et al., 2011); Crenarchaeol (V) and its regioisomer (VI) are produced only by thaumarchaea (de la Torre et al., 2008; Sinninghe Damsté et al., 2012). The relative abundance of specific iso GDGTs forms the basis of the TEX_{86} index (tetraether index of tetraethers consisting of 86 carbons; Schouten et al., 2002; Wuchter et al., 2004), which has been shown to correlate with sea surface temperature (SST; Schouten et al., 2002; Kim et al., 2008, 2010a) and lake surface temperature (Powers et al., 2004; Tierney et al., 2010), consistent with mesocosm culture experiments (Wuchter et al., 2004; Schouten et al., 2007). Because of the ubiquitous distribution of iso GDGTs, TEX_{86} values have been applied to infer

past changes in SST for a range of marine environments and temporal scales (e.g. Pagani et al., 2006; Sluijs et al., 2006; Weijers et al., 2007a; Liu et al., 2009). Apart from aquatic environments, dry and alkaline soils in China were also observed to contain significantly high amounts of iso GDGTs (Yang et al., 2012; Xie et al., 2012). TEX_{86} calculated temperatures for these soils did not correlate with MAT, which was suggested to result from difference in archaeal communities between soils and aquatic environments—soils containing group I.1b and group I.1c thaumarchaeota and aquatic environments containing predominantly group I.1a crenarchaeota (Yang et al., 2012). However, results from culture experiments with soil thaumarchaeota contradict this hypothesis, as both group I.1a and I.1b thaumarchaeota from soil exhibit TEX_{86} calculated temperatures that reasonably reflect the ambient temperatures (Sinninghe Damsté et al., 2012).

MAT and soil pH have been shown to be the primary environmental factors determining GDGT distributions in soils (Weijers et al., 2007c; Peterse et al., 2009, 2010). Weijers et al. (2007c) observed a correlation between the MBT index and precipitation amount that was interpreted to be a result of a covariance of MAT and precipitation amount. Peterse et al. (2012) also found an impact of precipitation amount on GDGT distribution in a globally distributed sample set. It was observed that, for alkaline soils from arid regions, the MBT/CBT calculated MAT was significantly (by ca. 20 °C) offset from actual MAT (Peterse et al., 2012). These observations point towards the importance of further investigation of the effect of precipitation on GDGT distribution in soils, as precipitation amount is a controlling factor for soil moisture, and soil moisture is one of the leading factors affecting microbial diversity and activity in soils (Liu et al., 2000; Chen et al., 2007).

To this end, we studied soil samples collected across two environmental transects in the USA with distinct precipitation characteristics—one across the east coast from Maine to Georgia and the other from the western states of Montana, Wyoming, Colorado and Utah—in order to determine if precipitation amount impacts on

GDGT distributions, and whether the correlation between MAT and soil GDGT distribution is valid for very different precipitation conditions.

2. Material and methods

2.1. Sample collection and weather data

Soil samples (34) were collected along an East Coast transect (ECT), from below 30 cm depth (Fig. 2). MAT at the sampling sites ranges from ca. 8–19 °C and annual precipitation from ca. 900 to 1600 mm (Table 1). Samples were generally loam, ranging from clayey to gravelly and, in a few places, sand or loamy sand. Bedrock type varied from sedimentary to igneous and metamorphic.

Samples (33) were also collected from a western transect (WT), from ca. 15 cm depth due to the generally shallow soil development across the WT (Fig. 2). MAT ranges from ca. 3–12 °C and annual precipitation from 140 to 680 mm. The soils were generally loam, ranging from clayey to gravelly with a similar variation in bedrock type, as observed at ECT sites. ECT soils were characterized by generally lower pH values and shallower water table than WT soils.

Samples were stored in Whirl Pak sample bags, freeze-dried using a Labconco freeze drier and stored at -21 °C until extraction. We obtained weather data from the PRISM climate group database of the Oregon State University (<http://prismmap.nacse.org/nn/>). Geographical coordinates for the sampling sites were entered into the PRISM data explorer to obtain T max annual, T min annual and annual precipitation amount. MAT was calculated by averaging T max annual and T min annual. Bedrock information was obtained from the United States Geological Survey Mineral Resources Program On-Line Spatial Data (Geological Data) and the soil information was obtained from the United States Department of Agriculture Natural Resources Conservation Service Web Soil Survey.



Fig. 2. Map showing locations for samples collected along both the western (WT) and east-coast (ECT) transects.

Table 1
Soil type and characteristics, bedrock type and weather data for sampling sites (“–” indicates unavailability of data).

Sample	Latitude	Longitude	MAT (°C)	Precipitation (mm yr ⁻¹)	Elevation (m)	Rock type	Soil type	pH	Slope (%)	Depth to water table (inches)
ECT1	43.09	-71.16	9.6	1606	312	Concord ggranite (tonalinite)	Gravelly fine sandy loam	4.8	8–15	>80
ECT2	43.73	-70.70	8.1	1543	448	Mudstone (primary) sandstone (secondary)	Peat	–	–	–
ECT3	45.00	-68.65	7.8	1289	185	Sandstone (secondary-quartzite)	Silt loam	5.1	–	0–12
ECT4	44.62	-69.01	8.2	1331	379	Slate (schist)	Fine sandy loam	4.8	3–8	18–26
ECT5	44.17	-69.41	8.5	1406	215	Devonian granite	Silt loam	5.1	3–8	12–30
ECT6	44.09	-70.28	8.4	1397	293	Marble (calc-silicate)	Sandy loam	5.3	0–8	18–36
ECT7	42.32	-71.46	10.2	1350	269	Biotite Granite	Fine sandy loam	5.3	3–8	18–21
ECT8	42.06	-71.78	9.8	1408	686	Scituate granite gneiss	Fine sandy loam, stony	4.8	3–8	>80
ECT9	41.78	-72.28	10.2	1382	301	Mica schist	Fine sandy loam	5.9	–	60–72
ECT10	41.75	-72.96	9.9	1544	1045	Schist-lower Ordov.	Gravelly fine sandy loam	5.5	3–15	>80
ECT11	41.57	-73.50	10.8	1421	511	Gneiss (amphibolite) Cambrian	Stony silt loam	6.2	8–15	18–36
ECT12	41.23	-74.18	11.0	1388	465	Pyrx-hbl-qtz-plag gneiss (mafic)	Fine sandy loam	5.3	8–15	>80
ECT13	40.75	-74.44	12.2	1313	269	Sandstone (secondary-siltstone)	Sandy loam	5.1	3–8	ca. 6–8
ECT14	40.39	-75.28	12.3	1345	544	Argillite (shale)	Silt loam	6.1	3–8	12–30
ECT15	40.19	-75.80	12.4	1273	554	Arkose (siltstone)	Silt loam	6.1	0–3	0–6
ECT16	39.99	-76.50	13.1	1194	341	Limestone (phyllite)	Silt loam	7.3	8–15	>80
ECT17	39.65	-76.76	12.6	1164	587	Schist (quartzite)	Sandy loam	5.8	25–45	>80
ECT18	38.76	-77.12	14.3	1108	97	Sand (clay or mud)	Loam	4.6	0–2	24–36
ECT19	38.34	-77.15	14.8	1119	103	Sand (silt)	Fine sandy loam, gravelly substratum	5.3	2–6	>80
ECT20	37.81	-77.12	15.1	1220	108	Sand (gravel)	Silty clay loam (mucky)	5.3	0–1	ca. 0
ECT21	37.36	-77.59	15.0	1243	292	Gravel (sand)-Tertiary	Sandy loam	5.5	6–12	>80
ECT22	36.84	-77.92	15.0	1247	358	Gneissic granite and granodiorite	Sandy clay loam	5.5	8–15	>80
ECT23	36.44	-78.37	15.2	1189	367	Granulite	Fine sandy loam	6.8	2–8	12–24
ECT24	35.95	-78.61	15.7	1183	200	Biotite gneiss (mica schist)	Sandy loam	5.5	6–10	>80
ECT25	35.46	-78.91	16.1	1110	390	Felsic gneiss (mafic gneiss)	Fine sandy loam	5.5	8–15	>80
ECT26	34.68	-78.60	17.0	1344	102	Clay or mud (sand)	Sand	5.1	0–3	0–12
ECT27	34.39	-79.00	17.2	1313	89	Clay or mud (sand)	Loamy sand	5.3	0–6	>80
ECT28	34.33	-79.26	17.3	1228	93	Sand (limestone)	Sand	5.3	0–6	>80
ECT29	33.95	-79.98	17.6	1195	197	Sand (limestone)	Sand	5.1	0–2	40–69
ECT30	33.52	-80.49	18.2	1101	220	Sand (clay or mud)	Loamy sand	5.6	0–6	>80
ECT31	33.06	-81.09	18.4	1014	123	Sand (clay or mud)	Sand	5.3	2–6	60–79
ECT32	32.88	-81.96	18.7	878	197	Sandstone (claystone)	Sand	5.5	0–5	48–60
ECT33	31.51	-82.76	19.2	918	205	Stream alluvium	Loamy sand	5.3	1–5	48–72
ECT34	31.03	-83.10	19.4	923	231	Sand (gravel)	Loamy sand	5.3	0–4	36–60
WT1	37.95	-107.84	3.2	513	2689	Permian sandstone	Gravelly loam	6.4	0–15	>80
WT2	40.17	-104.99	9.3	453	1748	Quaternary alluvium	Sandy loam	7.9	0–3	>80
WT3	40.84	-104.96	7.9	465	1722	Cretaceous sandstone	Sandy loam	7.2	3–9	>80
WT4	41.81	-104.80	7.5	553	1581	Oligocene White River Fm	Sandy loam	7.9	10–60	>80
WT5	42.34	-105.04	7.0	438	1528	White River Fm.	Fine sandy loam	7.9	6–50	>80
WT6	41.40	-104.86	6.8	514	1875	Sandstone/claystone (Upper Miocene)	Loam	7.6	0–6	>80
WT7	38.39	-108.96	10.6	244	1613	Triassis sandstone	Fine sandy loam	7.6	1–4	>80
WT8	38.22	-108.49	10.6	225	1805	Cretaceous sandstone	Loam to gravelly loam	7.9	5–30	>80
WT9	38.03	-108.11	6.7	323	2181	Cretaceous sandstone	Very stony clay loam	5.6	20–70	>80
WT10	45.67	-109.25	7.1	367	1159	Cretaceous shale	Clay and silt loam	7.5	4;15	>80
WT11	45.71	-110.40	7.1	393	1364	Livingston Fm. Tertiary volcanic	Cobbly clay to sandy loam	7.3	0–8	>80
WT12	45.50	-111.70	5.5	408	1746	Archean metamorphic	Gravelly sandy loam	7	15–45	>80
WT13	45.02	-112.25	4.2	424	2172	Tertiary sediment/volcanics	Silt, clay loam	6.7	2–15	>80
WT14	44.82	-113.25	3.1	432	2271	Tertiary sediments/volcanics	Gravelly clay, gravelly loam	6.3	20–50	12–24
WT16	42.80	-112.26	7.0	450	1412	Miocene basalt/Loess	Cobbly silt loam	7.5	4–12	>80
WT17	43.04	-112.21	6.5	580	1398	Miocene basalt/Loess	Very cobbly loam	7.9	4–20	>80
WT18	40.00	-111.41	7.1	581	1644	Cretaceous conglomerate	No information (Duchesne area, UT)	–	–	–
WT19	39.60	-110.83	8.8	171	1702	Cretaceous shale	Weathered bedrock (badland)	–	30–75	–
WT20	44.86	-112.50	3.4	450	2186	Tertiary volcanics	Gravelly sandy loam	7.6	8–35	>80

WT21	44.18	-112.24	5.5	255	1582	Miocene basalt/loess	No information (Clark County Area, ID)	-	-	-
WT22	43.41	-112.22	6.4	315	1442	Miocene basalt/loess	Silt loam	7.9	2-4	>80
WT23	41.58	-112.23	8.6	419	1359	Holocene lake deposits/salt flat	Silt loam	8	0-1	30-48
WT24	38.94	-109.82	11.8	143	1489	Cretaceous shale	Silt loam	8.5	0-3	>80
WT25	38.33	-109.43	10.4	236	1765	Jurassic sandstone	Very fine sandy loam	7.9	1-6	>80
WT26	40.98	-117.76	9.7	225	1341	Triassic claystone	Very fine sandy loam	7.5	8-15	>80
WT27	44.68	-106.87	6.5	476	1387	Eocene mudstone	Clay loam	7	9-15	>80
WT28	44.82	-107.34	5.2	540	1790	Devonian LS	No information (Big Horn National Forest, WY)	-	-	-
WT29	44.79	-107.39	3.0	680	2413	Archean granite	No information (Big Horn National Forest, WY)	-	-	-
WT30	44.79	-107.94	3.8	569	2437	Devonian LS	No information (Big Horn National Forest, WY)	-	-	-
WT31	45.21	-108.87	6.7	217	1191	Mowry shale	clay	7.5	-	>80
WT32	43.27	-106.39	6.5	276	1577	Cretaceous ss	Loam to sandy clay loam	8.5	2-12	>80
WT33	44.79	-107.98	3.8	569	1913	Triassic Chugwater Fm	No information (Big Horn County Area, WY)	-	-	-

2.2. Sample preparation

An aliquot (20–30 g) of freeze-dried soil was powdered and extracted using a Dionex ASE 300 accelerated solvent extractor with 9:1 CH₂Cl₂/MeOH (v/v). The total lipid extract (TLE) was concentrated under a stream of purified N₂ using a Zymark Turbovap II evaporator. Aliphatic, aromatic and polar fractions were obtained using column chromatography with deactivated silica gel (ca. 4 g; 70–230 mesh) in a baked Pasteur pipette, eluting sequentially with 2 ml hexane, 4 ml CH₂Cl₂ and 4 ml MeOH, respectively. The MeOH fraction, containing the GDGTs, was dried under purified N₂, dissolved in 1:1 CH₂Cl₂/MeOH (v/v) and passed through a column of activated basic Al₂O₃. The eluting fraction was then dried under N₂, dissolved in an azeotrope of hexane/isopropanol (99:1, v/v) and filtered through ashed a 0.7 μm glass microfiber filter.

2.3. GDGT analysis

Identification and quantification of GDGTs was conducted using high performance liquid chromatography–atmospheric pressure chemical ionization mass spectrometry (HPLC–APCI–MS; Agilent 1200 series Liquid Chromatograph–Single Quadrupole Mass Spectrometer), following methods described by Schouten et al. (2007). An Alltech Prevail Cyano column (150 mm, 2.1 mm i.d., 3 μm grain size) was used. The solvent gradient was: 100% A (hexane/isopropanol, 99:1, v/v; 5 min), then increasing the amount of B (hexane/isopropanol, 90:10, v/v) from 0% at 5 min to 7.4% at 40 min (held 10 min). The column was flushed with 100% B for 14 min in the back-flush mode, followed by 10 min equilibration with 100% A. Samples were scanned in selected ion monitoring (SIM) mode. Peak integration was carried out using Agilent Chemstation. Due to the lack of an appropriate internal standard, which could be added to the sample prior to processing for performing quantitative analysis, we were unable to determine GDGT concentration. We therefore report total peak areas divided by sample wt. (peak area g⁻¹ 10⁻³) to give an approximate idea of GDGT amount (as the dilution and injection amount were the same for all the samples) and also to be able to compare iso and br GDGT abundance in the soils.

2.4. Calculation of TEX₈₆, MBT, CBT, BIT and methane indices

Indices and temperature calibrations for TEX₈₆ (Powers et al., 2010) and MBT/CBT and BIT (Weijers et al., 2006a, 2007c) values were as follows.

$$\text{TEX}_{86} = (\text{II} + \text{III} + \text{IV}^*) / (\text{I} + \text{II} + \text{III} + \text{IV}^*) \quad (1)$$

$$\text{Temperature (ALST)} = -10.4 + 50.8 \times \text{TEX}_{86} \quad (2)$$

TEX₈₆ index was calculated from the relative abundances of iso GDGTs following Eq. (1) (Schouten et al., 2002). Eq. (2) represents the relationship between TEX₈₆ and temperature, in this case ALST or annual lake surface temperature, established by investigation of a globally distributed core top sample set by Powers et al. (2010). Iso GDGTs produced by thaumarchaea are abundant in marine and lacustrine sediments, so the TEX₈₆ index has been calibrated to sea and lake surface temperatures. We applied the TEX₈₆–ALST calibration, as no calibration has been established between TEX₈₆ and MAT or soil temperature.

Branched GDGTs are generally characteristic of soil and their abundances are used to calculate MBT and CBT indices [Eqs. (3) and (4), respectively; Weijers et al., 2007c]. MBT and CBT indices are used to calculate MAT, using a calibration [Eq. (5)] developed from a globally distributed soil sample set (Weijers et al., 2007c).

$$\text{MBT} = (\text{V} + \text{VI} + \text{VII}) / \{(\text{V} + \text{VI} + \text{VII}) + (\text{VIII} + \text{IX} + \text{X}) + (\text{XI} + \text{XII} + \text{XIII})\} \quad (3)$$

$$\text{CBT} = -\log\{(VI + IX)/(V + VIII)\} \quad (4)$$

$$\text{MAT} = (\text{MBT} - 0.122 - 0.187 \times \text{CBT})/0.02 \quad (5)$$

The BIT index [Eq. (6)] is an estimate of the relative abundance of iso and br GDGTs, with values ranging potentially from 0 to 1 (Weijers et al., 2006a). A BIT index value of 0 indicates a sample containing only iso GDGTs and that of 1 indicates the presence of only br GDGTs.

$$\text{BIT} = (V + VIII + XI)/(V + VIII + XI + IV) \quad (6)$$

The methane index [MI; Eq. (7)] is used to estimate the contribution of methane-oxidizing euryarchaea to the isoprenoid GDGTs (Zhang et al., 2011).

$$\text{MI} = (I + II + III)/(I + II + III + IV + IV^*) \quad (7)$$

3. Results

3.1. GDGT distributions

All the ECT samples contain commonly observed soil GDGT distributions, with br GDGTs dominant over iso GDGTs. Iso GDGTs were detected in only seven samples and generally represent < 1% of total GDGTs (Fig. 3c). In contrast, almost all WT soils contain iso GDGTs in unusually high abundance. In most cases, iso GDGTs dominate in WT soils (Fig. 3a and b). This is also evident in the total peak areas of both iso and br GDGTs divided by sample weight (Table 2). We report this as an approximation of GDGT amount as quantitative GDGT analysis was not performed. These values also indicate that, in general, GDGT content in the ECT soils is higher than in the WT soils. However, some of the WT and ECT soils are comparable in their GDGT concentrations (Table 2).

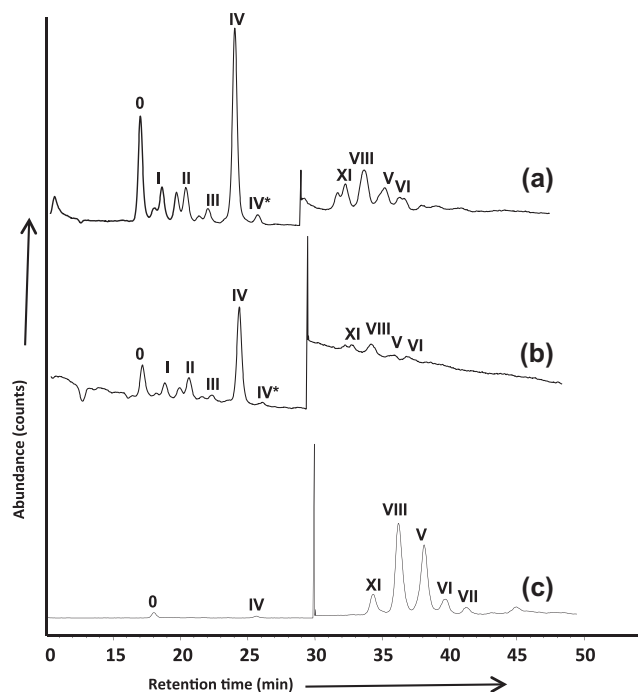


Fig. 3. GDGT distribution patterns in soils. SIM chromatograms from three representative soil samples from Montana, Colorado and east coast are shown in (a), (b) and (c), respectively. The chromatogram peaks are denoted by the GDGT numbers. At ca. 30 min the LC–MS method (SIM mode) was set up to change from scanning for isoprenoid GDGTs to scanning for branched GDGTs, which resulted in the observed jump in the chromatogram.

Both crenarchaeol (GDGT-IV) and caldarchaeol (GDGT-0) are present in very low amount in the ECT soils. The caldarchaeol/crenarchaeol ratio is used to estimate relative contribution of methanogenic euryarchaeotal and thaumarchaeotal lipids in sediments (Blaga et al., 2009), with a value > 2 indicating a significant contribution from methanogenic (and also methanotrophic) euryarchaeota (Blaga et al., 2009). Despite the low amount of iso GDGTs in the ECT soils, from comparing all the ECT samples, it appears that two have considerably higher caldarchaeol/crenarchaeol ratio (> 20) than the rest (Fig. 4a). Three other ECT soils have caldarchaeol/crenarchaeol values > 2 (Fig. 4a). In WT soils, caldarchaeol/crenarchaeol values slightly higher than 2 (2.65–4) were observed in only four samples (Fig. 4a).

3.2. MBT, CBT, TEX_{86} indices and temperature estimates

TEX_{86} , MBT, CBT and BIT data for all the samples are presented in Table 2. ECT samples display a moderate correlation between observed MAT and MBT indices (R^2 0.5, p -level < 0.01), while temperature calculated using MBT/CBT indices show a better correlation with measured MAT (R^2 0.7, p -level < 0.01; Fig. 5a and b). In contrast, MBT index values and temperature calculated using MBT/CBT indices for WT soils show no clear relationship with observed MAT (Fig. 5a and b). Many WT soils have abundant iso GDGTs that allow calculation of temperature using the lacustrine TEX_{86} -ALST calibration (Powers et al., 2010). We recognize that the lacustrine calibration is not valid for soil and no correlation was observed between measured MAT and TEX_{86} indices or TEX_{86} calculated temperature (Fig. 5c).

The total data show good correlation between MBT vs. measured MAT (Fig. 5a) and measured vs. calculated MAT (Fig. 5b), but significantly differ from regressions obtained when considering ECT soils alone. The difference between the regressions is statistically significant, as determined from ANCOVA test (the intercepts are statistically significantly different but the slopes are not). Moreover, the MBT vs. measured MAT correlation for the ECT soils is statistically significantly different from the correlation observed by Weijers et al. (2007c), but, when the total data are considered, the difference is not statistically significant.

3.3. BIT index

BIT index values for ECT soils range from 0.96 to 1 (Fig. 4b), while most WT soils show considerably lower BIT index values, ranging from 0 to 0.987 (Fig. 4b). BIT index values of all soils combined show a reasonably good correlation with precipitation (Fig. 5e).

4. Discussion

GDGT distributions between ECT and WT soils are clearly distinct, with the predominantly wet ECT soils displaying more typical soil GDGT distributions characterized by dominant br GDGTs (GDGT V–XII; Fig. 1) and the dry WT soils expressing patterns with iso GDGTs (GDGT I–IV; Fig. 1) commonly associated with marine or lake sediments. GDGT I, II and III can also be produced by methane oxidizing (methanotrophic) euryarchaea associated with methanogenic euryarchaea (Pancost et al., 2001; Blumenberg et al., 2004; Hopmans et al., 2004; Blaga et al., 2009; Zhang et al., 2011). The input of these compounds, which have no temperature relationship, has the potential to impact on TEX_{86} temperature estimates. Zhang et al. (2011) have developed an index for estimating contributions of GDGTs I–III from methane oxidizing (methanotrophic) euryarchaea, known as the MI, with values > 0.5 indicating an abundance of methane oxidizing euryarchaeal GDGTs. Further, the relative

Table 2

Relative abundance of isoprenoid and branched GDGTs, total peak areas of isoprenoid and branched GDGTs per g soil, caldarchaeol/crenarchaeol ratio, methane index, TEX₈₆ and calculated temperature, MBT, CBT and calculated MAT and pH, and BIT data.

Sample	Iso GDGT (%)	Br GDGT (%)	Total iso GDGT peak area (counts g ⁻¹ 10 ⁻³)	Total br GDGT peak area (counts g ⁻¹ 10 ⁻³)	R _i /R _b	Caldarchaeol/Crenarchaeol	Methane index	TEX ₈₆	TEX ₈₆ Temp (°C)	MBT	CBT	MAT-calculated (°C)	pH-calculated	BIT
ECT1	0	100	0	7265	0.000					0.77	1.92	14.5	3.7	1
ECT2	2.1	97.9	79	3711	0.021	3.7	0.42	0.58	18.8	0.49	1.03	8.9	6.1	1
ECT3	0.4	99.6	4	1047	0.004					0.54	1.42	7.8	5.0	1
ECT4	0	100	0	224	0.000					0.6	1.6	9.2	4.6	1
ECT5	0	100	0	619	0.000					0.56	1.53	7.4	4.7	1
ECT6	0	100	0	424	0.000					0.76	2.16	11.5	3.1	1
ECT7	0.7	99.3	2	275	0.007	0.4				0.72	1.13	19.1	5.8	0.99
ECT8	0.3	99.7	3	752	0.003			0.33	6.3	0.74	1.8	14.3	4.0	1
ECT9	5.2	94.8	12	224	0.054	26	0.86	0.53	16.4	0.59	1.17	12.6	5.7	1
ECT10	0.5	99.5	2	423	0.005			0.46	13.1	0.73	1.8	13.3	4.0	1
ECT11	0.2	99.8	1	700	0.002					0.72	1.97	11.5	3.6	1
ECT12	3.1	96.9	4	120	0.032	0.4				0.53	0.66	14.3	7.0	0.97
ECT13	0.9	99.1	4	427	0.009	0.9	0.56	0.66	23.1	0.65	1.52	12.3	4.8	1
ECT14	0.1	99.9	1	1443	0.001					0.7	1.81	12.1	4.0	1
ECT15	0.1	99.9	0.4	364	0.001					0.69	1.57	14.0	4.6	1
ECT16	4.0	96	2	46	0.041	0.2				0.63	0.84	17.6	6.6	0.96
ECT17	0.2	99.8	2	942	0.002			0.45	12.5	0.76	1.87	14.6	3.8	1
ECT18	0	100	0	91	0.000					0.61	1.37	11.8	5.2	1
ECT19	0.1	99.9	0.6	965	0.001					0.86	2.04	18.0	3.4	1
ECT20	2	98	2	86	0.020	0.9	0.42	0.51	15.6	0.79	1.9	15.6	3.7	0.99
ECT21	0.3	99.7	9	2904	0.003			0.48	14.0	0.87	1.83	20.3	3.9	1
ECT22	0	100	0	592	0.000					0.89	1.79	21.8	4.0	1
ECT23	0.2	99.8	0.2	127	0.002					0.83	1.76	19.2	4.1	1
ECT24	0	100	0	321	0.000					0.84	1.83	18.7	3.9	1
ECT25	0	100	0	277	0.000					0.9	1.83	21.7	4.0	1
ECT26	0.7	99.3	4	608	0.007			0.54	16.9	0.92	1.75	23.6	4.2	1
ECT27	0.4	99.6	1	338	0.004			0.54	17.1	0.84	1.55	21.4	4.7	1
ECT28	0.3	99.7	4	1263	0.003			0.57	18.7	0.89	1.76	21.8	4.1	1
ECT29	0.3	99.7	39	14220	0.003	21.5	0.94	0.68	24.2	0.92	1.86	22.5	3.9	1
ECT30	1.1	98.9	18	1669	0.011	1.8	0.74	0.62	21.2	0.86	1.87	19.3	3.8	1
ECT31	1.6	98.4	14	828	0.017	3.9	0.69			0.74	1.57	16.3	4.6	1
ECT32	0.3	99.7	2	756	0.003	0.8				0.75	1.04	21.5	6.0	1
ECT33	0.4	99.6	8	2304	0.004	6.3	0.90	0.62	21.2	0.9	2.09	19.3	3.3	1
ECT34	5.1	94.9	73	1349	0.054	0.4	0.22	0.75	27.8	0.7	0.62	23.4	7.1	0.96
WT1	73	27	46	17	2.71	0.8	0.30	0.6	19.9	0.14	0.49	-3.8	7.5	0.39
WT2	100	0	4	0	0.3		0.20	0.59	19.7					0
WT3	70.2	29.8	26	11	2.36	1	0.27	0.76	28.0	0.23	0.66	-0.6	7.0	0.48
WT4	80.4	19.6	14	3	4.09	0.8	0.24	0.76	28.2	0	0.9	-14.6	6.4	0.31
WT5	79.3	20.7	31	8	3.84	2.7	0.28	0.65	22.8	0.39	-0.03	13.6	8.8	0.38
WT6	83.9	16.1	2	0.4	5.22	0.6	0.32	0.72	26.1					0.3
WT7	76.4	23.6	31	10	3.24	0.5	0.30	0.69	24.6	0.09	1.04	-11.3	6.0	0.33
WT8	79.1	20.9	29	8	3.77	0.8	0.27	0.73	26.7	0.19	0.31	0.4	7.9	0.3
WT9	85	15	79	14	5.67	1.2	0.24	0.69	24.6	0.06	0.7	-9.6	6.9	0.29
WT10	79.6	20.4	116	30	3.89	0.4	0.25	0.78	29.3	0.09	0.67	-7.6	7.0	0.31
WT11	76	24	1070	337	3.17	0.4	0.23	0.81	30.6	0.09	0.59	-7.2	7.2	0.3
WT12	42.7	57.3	17	22	0.75	0.5	0.34	0.74	27.1	0.17	0.84	-5.6	6.5	0.71
WT13	62	38	26	16	1.63	0.8	0.28	0.65	22.7	0.14	0.42	-3.1	7.7	0.5
WT14	65.5	34.5	19	10	1.90	0.8	0.29	0.67	23.6	0.09	0.82	-9.5	6.6	0.49
WT16	86	14	771	125	6.15	3.3	0.29	0.66	23.2	0.09	0.62	-7.2	7.1	0.38
WT17	80	20	39	10	4.00	0.8	0.24	0.72	26.2	0				0.27
WT18	61.7	38.3	829	513	1.61	0.6	0.28	0.68	24.0	0.1	0.7	-7.3	6.9	0.49
WT19	72.2	27.8	2	0.6	2.59	2.2	0.33	0.63	21.4	0.54	0.68	14.8	7.0	0.54
WT20	73.5	26.5	10	4	2.77	4	0.23	0.73	26.5	0.39	-0.56	18.4	10.2	0.35
WT21	73.6	26.4	185	66	2.78	0.3	0.22	0.78	29.4	0.03				0.34
WT22	62.9	37.1	538	317	1.70	0.2	0.21	0.71	25.7	0.11	0.7	-7.1	6.9	0.45
WT23	63.9	36.1	285	161	1.77	0.7	0.30	0.65	22.6	0.09	1.6	-16.6	4.6	0.54
WT24	88.8	11.2	5	0.6	7.91	0.7	0.25	0.71	25.7	0				0.21
WT25	85.8	14.2	6	1	6.045	0.6	0.33	0.71	25.5	0.05				0.26
WT26	94.4	5.6	1	0.1	16.83	0.4	0.25	0.7	25.0	0				0.1
WT27	71.7	28.3	614	242	2.54	0.4	0.27	0.75	27.9	0.03	1.17	-15.4	5.7	0.41
WT28	1.8	98.2	80	4261	0.02	0.2	0.29	0.79	29.9	0.15	0.57	-3.7	7.3	0.99
WT29	27	73	1	2	0.37		0.69	0.38	8.7	0.19	1.25	-8.1	5.5	0.9
WT30	33.9	66.1	49	95	0.51	0.7	0.35	0.66	23.0	0.15	0.36	-1.8	7.8	0.77
WT31	90.9	9.1	11	1	10.02	0.9	0.31	0.66	23.3	0.03				0.19
WT32	88.2	11.8	40	5	7.50	0.4	0.18	0.95	38.1	0				0.16
WT33	83.1	16.9	47	10	4.92	0.3	0.22	0.77	28.6	0				0.22

abundance of caldarchaeol and crenarchaeol, expressed by the caldarchaeol/crenarchaeol ratio has been applied as an alternative indicator of a euryarchaeotal (methanogenic and methanotrophic)

contribution (Blaga et al., 2009). While caldarchaeol (GDGT-0) is synthesized by methanogenic euryarchaea, crenarchaeol is synthesized only by thaumarchaea (de la Torre et al., 2008; Sinninghe

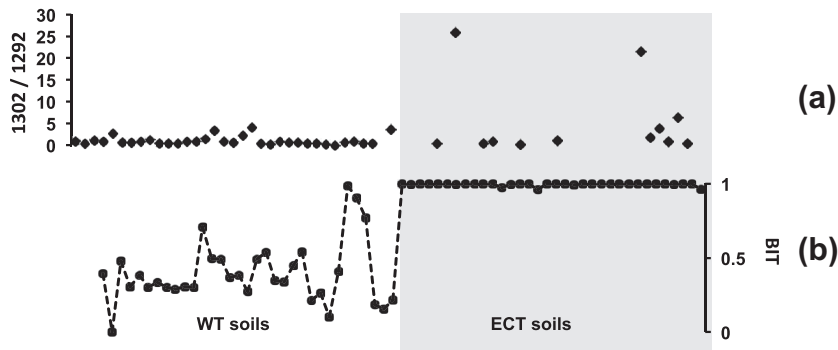


Fig. 4. Illustration of contrasting GDGT distribution patterns in the ECT and WT soils. Shaded area represents samples from the ECT and non-shaded area samples from WT. Caldarchaeol/crenarchaeol values (1302/1292) are shown in (a) and BIT indices in (b).

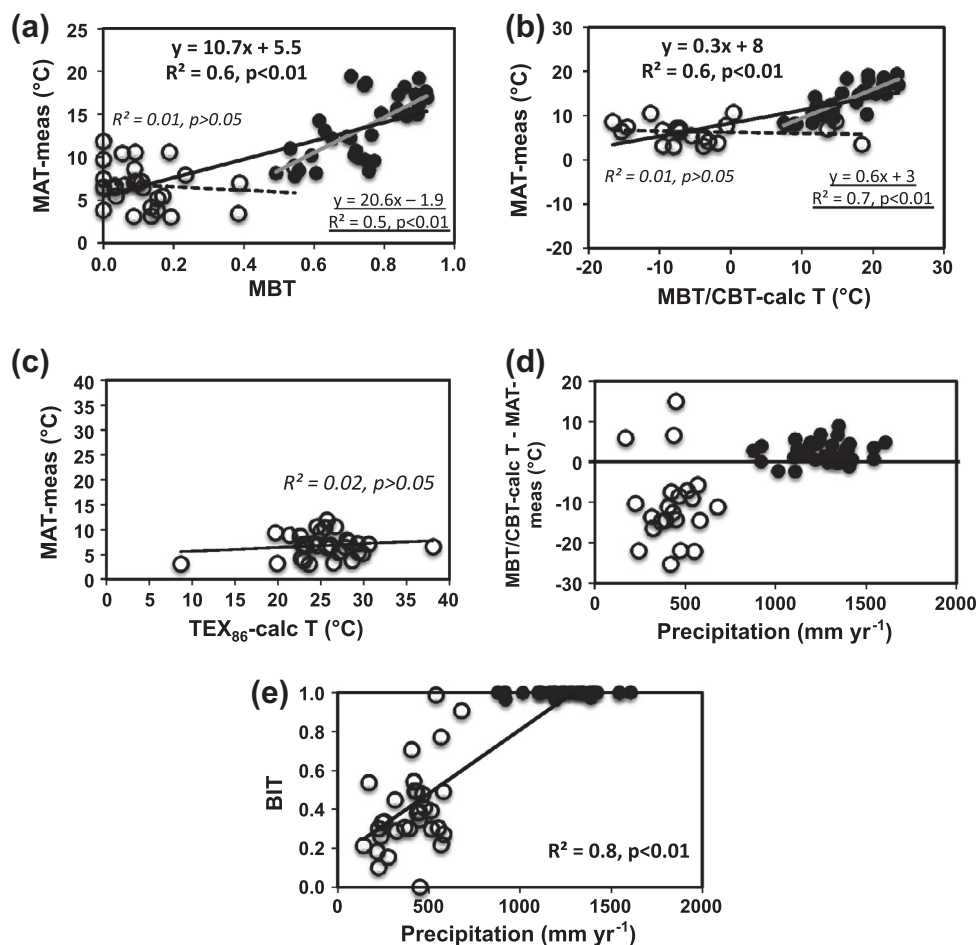


Fig. 5. (a) Correlation between measured MAT (°C) and MBT from all the soil samples (filled circles represent ECT soils and open circles WT soils; dotted line represents individual correlation for WT soils, the R^2 value and p -level for which are shown in italics; gray line represents individual correlation for ECT soils, the equation, R^2 value and p -level for which are underlined, and the black line the correlation for all the soils combined, the equation, R^2 value and p -level for which are shown in bold). (b) Correlation between measured MAT (°C) and MBT/CBT calculated MAT (°C) from all soils, combining WT and ECT [symbols and correlations are as in (a)], the offset between the correlation for ECT soils (gray line) and the 1:1 line probably resulting from the calibration error involved in the estimation of MAT (Schouten et al., 2013). (c) Correlation between measured MAT (°C) and calculated temperature (°C) using TEX_{86} from WT soils. (d) Difference between measured MAT and MBT/CBT calculated MAT (calculated by subtracting the calculated temperature from measured MAT) with precipitation from all soils [ECT and WT soils are represented by same symbols as in (a)]. (e) Correlation between BIT index measured from all the soils and precipitation from all soils [ECT and WT soils are represented by same symbols as in (a)].

Damsté et al., 2012). A caldarchaeol/crenarchaeol ratio > 2 indicates methanogenic activity in soils, sediments or particulate matter (Blaga et al., 2009). Methanogenic activity is very common in wetland and peat sediments (Ferry and Kestead, 2007), but also occurs in soils under anoxic conditions (Ferry and Kestead, 2007) or

in the presence of anoxic microenvironments in soils or sediments (Großkopf et al., 1998; West and Schmidt, 2002; Angel et al., 2012). Organic matter (OM) in these environments is converted to acetate and formate and to CO_2 and H_2 by fermentative bacteria under anoxic conditions and these products are then converted to CH_4 by

methanogenic archaea and subsequently metabolized by methanotrophic archaea. These GDGT distributions are clear indicators of methanogenic activity and, if detected, void the application of GDGTs as a temperature indicator.

4.1. East Coast transect

The detection of GDGTs I–IV (Fig. 3c) in very low amount (< 1% on average) in some of the ECT soils (14 out of 34 samples) indicates an input from thaumarchaea. In spite of their small amounts, we estimated caldarchaeol/crenarchaeol ratios and MI values. Six of the ECT soils have MI > 0.5, indicating the presence of methane oxidizing euryarchaea (Table 2) and two have caldarchaeol/crenarchaeol values > 20, indicating significant activity of methanogenic archaea (Fig. 4a), in turn pointing towards the presence of anoxic conditions at these locations. Only two of the east coast sampling locations are characterized by the presence of peat or mucky deposits, but, surprisingly, none of these display high caldarchaeol/crenarchaeol values. There is no direct evidence of methanogenic activity in the other soils.

In general, soils are characterized by the presence and dominance of br GDGTs (GDGTs V–XIII; Weijers et al., 2006a, 2007c) likely synthesized by facultative anaerobic heterotrophic acidobacteria (Hopmans et al., 2004; Weijers et al., 2004, 2006b, 2010). Thus, the dominance of br GDGT-V to GDGT-XIII in the ECT soils (Figs. 3c and 4b) indicates the presence of anoxic conditions in these soils and, for some localities, caldarchaeol/crenarchaeol values and MI values indicate methanogenic metabolism. Anoxic conditions in these soils would be expected, given the high amount of precipitation, as opposed to the dry WT soils, where oxic conditions may have led to a distinctly different GDGT distribution pattern (Cleveland et al., 2010). MBT index values calculated from the ECT soils correlate moderately with measured MAT (R^2 0.5, p -level < 0.01; Fig. 5a) and MBT/CBT calculated temperature from ECT soils also correlates well with measured MAT (R^2 0.7, p -level < 0.01; Fig. 5b).

4.2. Western transect

In contrast to the ECT soils, most WT samples contain significantly high abundances of iso GDGTs relative to br GDGTs (Fig. 3a and b), with 71% of total GDGTs on average (ranging from ca. 21% to 100%) for all WT soils represented by iso GDGTs. However, the relative abundances were calculated only on the basis of peak areas, not absolute abundance. The BIT values for the WT soils ranged from ca. 0.2 to 0.7 and the average BIT index for all the WT soils is 0.39. BIT values as low as ca. 0.2 are occasionally observed in soils (Schouten et al., 2013; Yang et al., 2012; Xie et al., 2012). It must also be noted that instrumental difference in laboratories is also an important factor contributing to the differences in BIT values reported in various studies (Schouten et al., 2009, 2013). Importantly, a high abundance of iso GDGTs occurs in soils developed on strictly non-marine continental sedimentary or igneous rock at some locations, in contrast to current expectations of iso GDGTs associated with marine and lacustrine environments. Although thaumarchaeotal iso lipids are common in soils (Weijers et al., 2006a; Schouten et al., 2013), their abundance is generally much lower than those observed here in WT soils and in dry, alkaline soils from China (Yang et al., 2012; Xie et al., 2012). The abundance of only the three major br GDGTs, i.e. m/z 1050, m/z 1036 and m/z 1022 (GDGT-V, VIII, and XI) was reported by Weijers et al. (2006a), but these three compounds constitute the bulk of br GDGTs in soils. Considering only these three major br GDGTs, the abundance of iso GDGTs in the globally distributed sample set studied by Weijers et al. (2006a) was 25% on average (ranging from 2% to 54%). If the six other br GDGTs were included in the cal-

ulation, the relative proportion of iso GDGTs in these soils would be even lower. Interestingly, the high abundance of iso GDGTs easily facilitates calculation of TEX_{86} index values from the WT soils, which is not common for soils (Fig. 5c). A similar GDGT distribution in soil, characterized by more abundant iso GDGTs than br GDGTs, has recently been reported in modern soil samples from China (Xie et al., 2012; Yang et al., 2012). The authors expressed the relative abundance of iso and br tetraether lipids in terms of an iso/br ratio ($R_{i/b}$). In the Chinese soil samples, $R_{i/b}$ was very low (ca. 0.01–0.2) in acidic soils with > 600 mm mean annual precipitation (Xie et al., 2012). $R_{i/b}$ increased in alkaline, dry soils with < 600 mm mean annual precipitation, reaching up to ca. 7 (Xie et al., 2012). $R_{i/b}$ values for the WT soils range from ca. 0.02 to 17, with an average of 4 (Table 2). In contrast, in the ECT soils, $R_{i/b}$ ranges from 0 to 0.05 (Table 2).

4.3. Origin of different GDGT distribution patterns in ECT and WT

4.3.1. Differences in climatic conditions and soil characteristics

Differences between weather and soil characteristics of the ECT and WT soils can help explain the unusual distribution of GDGTs in the WT soils. The most prominent difference between ECT and WT is mean annual precipitation amount which, in ECT ranges from 900 to 1600 mm and in WT from 140 to 680 mm, and soil pH, with WT soils characterized by higher pH than ECT soils. Depth to the water table in WT soils was generally greater than ECT—likely a result of drier conditions across WT sites, as well as more porous, thinly mantled soils. Weijers et al. (2006a) observed low BIT values for soils, with the lowest values at the surface and increasing with depth. The lowest BIT value in the globally distributed sample set is 0.52 (Weijers et al., 2006a). Many of these soils are characterized by a relatively high concentration of crenarchaeol and weak correlation between relative abundance of crenarchaeol and pH (Weijers et al., 2006a). However, in the entire sample set, only three samples showed low BIT values, and these were located at the top layers of soil, which could potentially be indicative of a relationship between the degree of soil aeration and the relative abundances of iso and br GDGTs (Weijers et al., 2006b). Because br GDGT-producing organisms are facultative anaerobes, it is possible that depth of sampling plays a role in the relative abundance of br and iso GDGTs. Indeed, an increase in the concentration of br GDGTs has been observed in the anoxic zone of peat deposits, where the obligate anaerobic bacteria producing br GDGTs can thrive (Weijers et al., 2004). In oxidized environments, anaerobic bacteria can survive in anaerobic microenvironments, similar to methanogenic archaea, but in low abundance (West and Schmidt, 2002; Weijers et al., 2006a). However, as only very few samples had low BIT values in the sample set analyzed by Weijers et al. (2006a), the average BIT of all the samples reported by Weijers et al. (2006a) was 0.91—still substantially higher than in our study. Besides soil aeration, soil pH can be another important controlling factor affecting GDGT distribution in soils, and resulting in BIT values as low as ca. 0.2 in soils, as observed in later studies (Schouten et al., 2013 and references therein).

WT soils characterized by low BIT values could be explained in part by a high degree of soil aeration. Regions with low precipitation amount support high O_2 concentration in soils (Cleveland et al., 2010), leading to conditions unfavorable for br GDGT-producing anaerobic bacteria and, subsequently, a low concentration of br GDGTs. Average annual precipitation for the WT and ECT locations is ca. 403 mm and ca. 1255 mm, respectively (calculated from precipitation data obtained using the PRISM data explorer; see Section 2). Lower precipitation amount leads to low soil water content and high aeration (Picek et al., 2000; Davidon et al., 2004, 2008; Hossain and Uddin, 2011), promoting oxic conditions unfavorable for anaerobic bacteria. Further, the difference between measured

MAT and MBT/CBT-calculated temperatures indicates a relationship with regional precipitation (Fig. 5d). Above a mean annual precipitation (MAP) of 800 mm, offsets range from -5°C to 9°C and substantially increase as MAP falls below 800 mm (ranging from -25°C to 15°C) making MBT/CBT temperature estimates unreliable, which agrees with recent soil calibrations (Peterse et al., 2012).

Another explanation could be the effect of soil pH on the abundance of acidobacteria in soils, with corresponding changes in br GDGT concentration (Peterse et al., 2010). A negative correlation between soil pH and BIT indices has been observed at some locations, with BIT values decreasing with increasing pH (Kim et al., 2010b; Schouten et al., 2013; Yang et al., 2012). Low BIT values have been reported from dry and alkaline Chinese soils (Yang et al., 2012; Xie et al., 2012). This negative correlation between soil pH and the abundance of acidobacteria, i.e. increasing pH leading to a decrease in the abundance of acidobacteria (Peterse et al., 2010) may also have led to the dry, alkaline WT soils being characterized by a lower abundance of br GDGTs.

4.3.2. Possible ancient origin of GDGTs

One factor which also needs to be considered, is the possibility that the GDGTs in WT soils were not synthesized under modern conditions and derive from the weathering flux of older sediments or sedimentary rocks (bedrock), which could be confirmed by compound specific radiocarbon dating not performed in this study. However, many of the WT locations are underlain by sedimentary bedrock—Tertiary continental sediments, Mesozoic sandstones, or igneous rocks which should not preserve any significant marine-derived iso GDGTs (Table 1). Only a few sites (< 5) are underlain by Mesozoic shales that could potentially contribute marine OM. Accordingly, we do not consider WT bedrock a significant source of GDGTs for several reasons. First, WT GDGTs are remarkably well preserved, contrary to expectation, given results from turbidite sediments (Huguet et al., 2008) that show all GDGTs decayed in the oxic parts of turbidites and autochthonous iso GDGTs decayed more rapidly than allochthonous br GDGTs, due to the protection of the branched GDGTs by matrix material, with a consequent increase in BIT index (Huguet et al., 2008). Similar GDGT amounts were observed for some WT and ECT soils. Thus, an allochthonous origin of GDGTs in WT soils would require a relatively high amount of GDGTs transported from the parent rock. It would also require a relatively high degree of preservation under the oxic conditions prevailing in WT soils. Further, two WT soils with low BIT index (ca. 0.3) are underlain by igneous bedrock. Moreover, the low BIT indices of WT soils cannot be explained by a mechanism involving preferential preservation of br GDGTs as observed for turbidites, which should result in an increase in BIT values (Huguet et al., 2008). These observations point towards an in situ origin of the iso GDGTs in these soils. Therefore, we conclude that WT iso GDGTs are autochthonous, i.e. produced in situ.

4.3.3. Thaumarchaeal communities in soils

Crenarchaeol and its regioisomer are abundant in WT soils, indicating the presence of thaumarchaea. Indeed, the presence of such organisms in dry soils has been reported (Timonen and Bomberg, 2009 and references therein). Thaumarchaea belonging to Group I.1b have been reported in soils with $\text{pH} > 5$ (Timonen and Bomberg, 2009). Therefore, Group I.1b thaumarchaea most likely inhabit WT soils, which are characterized by $\text{pH} > 5$ (Table 1). Two strains of group I.1b thaumarchaea from soils have been observed to synthesize crenarchaeol and its regioisomer by Sinninghe Damsté et al. (2012). Interestingly, group I.1b thaumarchaea synthesized significantly higher amounts of the regioisomer than group I.1a thaumarchaea (Sinninghe Damsté et al., 2012). Our conclusion is supported by the hypothesis proposed by Xie et al.

(2012) to explain the iso and br GDGT distribution patterns in Chinese soils mentioned above. According to Xie et al. (2012), dry alkaline soils promote NH_3 oxidation, whereas acidic wet soils hinder NH_3 oxidation by preventing the conversion of NH_4^+ to NH_3 . Thaumarchaea producing the iso GDGTs in soils are ammonia oxidizers. As a result, such ammonia oxidizing thaumarchaea will grow well in dry alkaline soils. On the other hand, acidic conditions in soils will be favorable for the br GDGT producing acidobacteria (Weijers et al., 2006b, 2010).

4.4. Implications for paleoclimatological studies

Using WT soil GDGTs, TEX_{86} , MBT/CBT indices and corresponding temperatures were calculated (Table 2). TEX_{86} calculated temperature was significantly higher (avg. 18.5°C) and MBT/CBT – calculated temperature lower (avg. 10°C) than measured MAT at the sample locations. Therefore, regardless of whether WT GDGTs are autochthonous or allochthonous, soil erosion from these and similar environments will introduce iso GDGTs into lacustrine environments and confound TEX_{86} temperature estimates, providing spurious estimates of soil carbon delivery. A similar situation may also occur in river dominated marginal sediments, where input of GDGTs from dry alkaline soils via soil erosion will not be detectable from BIT indices. Moreover, input from low BIT soils to lacustrine or shallow marine environments will also constrain the application of BIT indices in sediments to detect marine and terrestrial input in paleoclimatological studies.

5. Conclusions

Soils collected across six western US states contain an unusually high amount of isoprenoid GDGTs, accompanied by a low abundance of branched GDGTs and the lowest BIT index values measured to date. Soils from a north–south transect along the east coast of the US show GDGT distributions similar to previous studies of moist environments and are characterized by high BIT index values. Below an annual precipitation of ca. 800 mm, the MBT/CBT calculated MAT ($^{\circ}\text{C}$) shows a significantly higher offset from measured MAT than wetter sites—indicating a control of precipitation amount on the accurate applicability of the MBT/CBT temperature proxy. BIT index values for the soils show a relationship with mean annual precipitation, which has not been reported before. Input of GDGTs from soils with low BIT index values to lakes or marginal marine sediments may interfere with the temperature estimates from these sediments and go undetected by the BIT index. This also points towards a limitation in the application of BIT indices to ancient sediments for discriminating between marine and terrestrial contributions. Therefore, the use of GDGTs for paleotemperature studies requires examination of GDGT distributions in the surrounding soils. This is most critical for environments that have undergone significant paleoclimatic change that resulted in varying precipitation and rate of soil development.

Acknowledgements

We would like to thank two anonymous reviewers for comments that were helpful for improving the manuscript. The research was partly funded by the Yale University John F. Enders Fellowship and Research Grant.

Associate Editor – S. Schouten

References

Affek, H.P., Bar-Matthews, M., Ayalon, A., Matthews, A., Eiler, J.M., 2008. Glacial/interglacial temperature variations in Soreq cave speleothems as recorded by

- 'clumped isotope' thermometry. *Geochimica et Cosmochimica Acta* 72, 5351–5360.
- Angel, R., Claus, P., Conrad, R., 2012. Methanogenic archaea are globally ubiquitous in aerated soils and become active under wet anoxic conditions. *The ISME Journal* 6, 847–862.
- Blaga, C.I., Reichart, G.J., Heiri, O., Sinninghe Damsté, J.S., 2009. Tetraether membrane lipid distributions in water-column particulate matter and sediments: a study of 47 European lakes along a north–south transect. *Journal of Paleolimnology* 41, 523–540.
- Blumenberg, M., Seifert, R., Reitner, J., Pape, T., Michaelis, W., 2004. Membrane lipid patterns typify distinct anaerobic methanotrophic consortia. *Proceedings of the National Academy of Sciences of the USA* 101, 11111–11116.
- Chen, M.-M., Zhu, Y.-G., Chen, B.-D., Fu, B.-J., Marschner, P., 2007. Effects of soil moisture and plant interactions on the soil microbial community structure. *European Journal of Soil Biology* 43, 31–38.
- Cleveland, C.C., Wieder, W.R., Reed, S.C., Townsend, A.R., 2010. Experimental drought in a tropical rain forest increases soil carbon dioxide losses to the atmosphere. *Ecology* 91, 2313–2323.
- Conte, M.H., Sicre, M.-A., Rühlmann, C., Weber, J.C., Schulte, S., Schulz-Bull, D., Blanz, T., 2006. Global temperature calibration of the alkenone unsaturation index (U_{37}^K) in surface waters and comparison with surface sediments. *Geochemistry Geophysics Geosystems* 7, Q02005. <http://dx.doi.org/10.1029/2005GC001054>.
- Davidson, E.A., Ishida, F.Y., Nepstad, D.C., 2004. Effects of an experimental drought on soil emissions of carbon dioxide, methane, nitrous oxide, and nitric oxide in a moist tropical forest. *Global Change Biology* 10, 718–730.
- Davidson, E.A., Nepstad, D.C., Ishida, F.Y., Brando, P.M., 2008. Effects of an experimental drought and recovery on soil emissions of carbon dioxide, methane, nitrous oxide, and nitric oxide in a moist tropical forest. *Global Change Biology* 14, 2582–2590.
- de la Torre, J.R., Walker, C.B., Ingalls, A.E., Könneke, M., Stahl, D.A., 2008. Cultivation of a thermophilic ammonia oxidizing archaeon synthesizing crenarchaeol. *Environmental Microbiology* 10, 810–818.
- Donders, T.H., Weijers, J.W.H., Munsterman, D.K., Hove, M.L.K., Buckles, L.K., Pancost, R.D., Schouten, S., Sinninghe Damsté, J.S., Brinkhuis, H., 2009. Strong climate coupling of terrestrial and marine environments in the Miocene of northwest Europe. *Earth and Planetary Science Letters* 281, 215–225.
- Epstein, S., Buchsbaum, R., Lowenstam, H.A., Urey, H.C., 1953. Revised carbonate–water isotopic temperature scale. *Geological Society of America Bulletin* 64, 1315–1325.
- Ferry, J.G., Kastead, K.A., 2007. Methanogenesis. In: Cavicchioli, R. (Ed.), *Archaea: Molecular Cell Biology*. ASM Press, Washington, DC, pp. 288–314.
- Ghosh, P., Garzzone, C.N., Eiler, J.M., 2006. Rapid uplift of the Altiplano revealed through ^{13}C – ^{18}O bonds in paleosol carbonates. *Science* 311, 511–515.
- Ghosh, P., Eiler, J., Campana, S.E., Feeney, R.F., 2007. Calibration of the carbonate 'clumped isotope' paleothermometer for otoliths. *Geochimica et Cosmochimica Acta* 71, 2736–2744.
- Großkopf, R., Janssen, P.H., Liesack, W., 1998. Diversity and structure of the methanogenic community in anoxic rice paddy soil microcosms as examined by cultivation and direct 16S rRNA gene sequence retrieval. *Applied and Environmental Microbiology* 64, 960–969.
- Herbert, T.D., Peterson, L.C., Lawrence, K.T., Liu, Z., 2010. Tropical ocean temperatures over the past 3.5 million years. *Science* 328, 1530–1534.
- Hopmans, E.C., Weijers, J.W.H., Schefuß, E., Herfort, L., Sinninghe Damsté, J.S., Schouten, S., 2004. A novel proxy for terrestrial organic matter in sediments based on branched and isoprenoid tetraether lipids. *Earth and Planetary Science Letters* 224, 107–116.
- Hossain, M.A., Uddin, S.N., 2011. Mechanisms of waterlogging tolerance in wheat: morphological and metabolic adaptations under hypoxia or anoxia. *Australian Journal of Crop Science* 5, 1094–1101.
- Hren, M.T., Pagani, M., Erwin, D.M., Brandon, M., 2010. Biomarker reconstruction of the early Eocene paleogeography and paleoclimate of the northern Sierra Nevada. *Geology* 38, 7–10.
- Huguet, C., de Lange, G.J., Gustafsson, Ö., Middelburg, J.J., Sinninghe Damsté, J.S., Schouten, S., 2008. Selective preservation of soil organic matter in oxidized marine sediments (Madeira Abyssal Plain). *Geochimica et Cosmochimica Acta* 72, 6061–6068.
- Huguet, A., Fosse, C., Metzger, P., Fritsch, E., Derenne, S., 2010. Occurrence and distribution of extractable glycerol dialkyl glycerol tetraethers in podzols. *Organic Geochemistry* 41, 291–301.
- Kennett, J.P., Shackleton, N.J., 1975. Laurentide ice sheet meltwater recorded in Gulf of Mexico deep-sea cores. *Science* 188, 147–150.
- Kim, J.-H., Schouten, S., Hopmans, E.C., Donner, B., Sinninghe Damsté, J.S., 2008. Global sediment core-top calibration of the TEX_{86} paleothermometer in the ocean. *Geochimica et Cosmochimica Acta* 72, 1154–1173.
- Kim, J.-H., van der Meer, J., Schouten, S., Helmke, P., Willmott, V., Sangiorgi, F., Koç, N., Hopmans, E.C., Sinninghe Damsté, J.S., 2010a. New indices and calibrations derived from the distribution of crenarchaeal isoprenoid tetraether lipids: implications for past sea surface temperature reconstructions. *Geochimica et Cosmochimica Acta* 74, 4639–4654.
- Kim, J.-H., Zarzycka, B., Buscail, R., Peterse, F., Bonnin, J., Ludwig, W., Schouten, S., Sinninghe Damsté, J.S., 2010b. Contribution of river-borne soil organic carbon to the Gulf of Lions (NW Mediterranean). *Limnology and Oceanography* 55, 507–518.
- Lear, C.H., Elderfield, H., Wilson, P.A., 2000. Cenozoic deep-sea temperatures and global ice volumes from Mg/Ca in benthic foraminiferal calcite. *Science* 287, 269–272.
- Lear, C.H., Rosenthal, Y., Slowey, N., 2002. Benthic foraminiferal Mg/Ca-paleothermometry: a revised core-top calibration. *Geochimica et Cosmochimica Acta* 66, 3375–3387.
- Leininger, S., Ulrich, T., Schlöter, M., Schwark, L., Qi, J., Nicol, G.W., Prosser, J.I., Schuster, S.C., Schleper, C., 2006. Archaea predominate among ammonia-oxidizing prokaryotes in soils. *Nature* 442, 806–809.
- Liu, Z., Herbert, T.D., 2004. High-latitude influence on the eastern equatorial Pacific climate in the early Pleistocene epoch. *Nature* 427, 720–723.
- Liu, X.Y., Lindemann, W.C., Whitford, W.G., Steiner, R.L., 2000. Microbial diversity and activity of disturbed soil in the northern Chihuahuan Desert. *Biology and Fertility of Soils* 32, 243–249.
- Liu, Z., Pagani, M., Zinniker, D., DeConto, R., Huber, M., Brinkhuis, H., Shah, S.R., Leckie, R.M., Pearson, A., 2009. Global cooling during the Eocene–Oligocene climate transition. *Science* 323, 1187–1190.
- Loomis, S., Russell, J., Sinninghe Damsté, J.S., 2011. Distributions of branched GDGTs in soils from western Uganda and implications for a lacustrine paleothermometer. *Organic Geochemistry* 42, 739–751.
- Müller, P.J., Kirst, G., Ruhland, G., von Storch, I., Rosell-Melé, A., 1998. Calibration of the alkenone paleotemperature index (U_{37}^K) based on core-tops from the eastern South Atlantic and the global ocean (60°N–60°S). *Geochimica et Cosmochimica Acta* 62, 1757–1772.
- Mutterlose, J., Malkoc, M., Schouten, S., Sinninghe Damsté, J.S., Forster, A., 2010. TEX_{86} and stable $\delta^{18}\text{O}$ paleothermometry of early Cretaceous sediments: implications for belemnite ecology and paleotemperature proxy application. *Earth and Planetary Science Letters* 298, 286–298.
- Nürnberg, D., Levitan, M.A., Pavlidis, J.A., Shelekova, E.S., 1995. Distribution of clay minerals in surface sediments from the eastern Barents and South-Western Kara seas. *Geologische Rundschau* 84, 665–682.
- Oppermann, B.I., Michaelis, W., Blumenberg, M., Frerichs, J., Schulz, H.M., Schippers, A., Beaubien, S.E., Krüger, M., 2010. Soil microbial community changes as a result of long-term exposure to a natural CO_2 vent. *Geochimica et Cosmochimica Acta* 74, 2697–2716.
- Pagani, M., Pedentchouk, N., Huber, M., Sluijs, A., Schouten, S., Brinkhuis, H., Sinninghe Damsté, J.S., Dickens, G.R., the Expedition 302 Scientists, 2006. Arctic hydrology during global warming at the Palaeocene/Eocene thermal maximum. *Nature* 442, 671–675.
- Pancost, R.D., Hopmans, E.C., Sinninghe Damsté, J.S., the MEDINAUT Shipboard Scientific Party, 2001. Archaeal lipids in Mediterranean Cold Seeps: molecular proxies for anaerobic methane oxidation. *Geochimica et Cosmochimica Acta* 65, 1611–1627.
- Pancost, R.D., Sinninghe Damsté, J.S., 2003. Carbon isotopic compositions of prokaryotic lipids as tracers of carbon cycling in diverse settings. *Chemical Geology* 195, 29–58.
- Pester, M., Schleper, C., Wagner, M., 2011. The Thaumarchaeota: an emerging view of their phylogeny and ecophysiology. *Current Opinion in Microbiology* 14, 300–306.
- Peterse, F., Kim, J.-H., Schouten, S., Kristensen, D.K., Koç, N., Sinninghe Damsté, J.S., 2009. Constraints on the application of the MBT/CBT paleothermometer at high latitude environments (Svalbard, Norway). *Organic Geochemistry* 40, 692–699.
- Peterse, F., Nicol, G.W., Schouten, S., Sinninghe Damsté, J.S., 2010. Influence of soil pH on the abundance and distribution of core and intact polar lipid-derived branched GDGTs in soil. *Organic Geochemistry* 41, 1171–1175.
- Peterse, F., van der Meer, J., Schouten, S., Weijers, J.W.H., Fierer, N., Jackson, R.B., Kim, J.-H., Sinninghe Damsté, J.S., 2012. Revised calibration of the MBT–CBT paleotemperature proxy based on branched tetraether membrane lipids in surface soils. *Geochimica et Cosmochimica Acta* 96, 215–229.
- Picek, T., Simek, M., Santruckova, H., 2000. Microbial responses to fluctuation of soil aeration status and redox conditions. *Biology and Fertility of Soils* 31, 315–322.
- Podlaha, O.G., Mutterlose, J., Veizer, J., 1998. Preservation of $\delta^{18}\text{O}$ and $\delta^{13}\text{C}$ in belemnite rostra from the Jurassic/Early Cretaceous successions. *American Journal of Science* 298, 324–347.
- Powers, L.A., Werne, J.P., Johnson, T.C., Hopmans, E.C., Sinninghe Damsté, J.S., Schouten, S., 2004. Crenarchaeotal membrane lipids in lake sediments: a new paleotemperature proxy for continental paleoclimate reconstruction? *Geology* 32, 613–616.
- Powers, L., Werne, J.P., Vanderwoude, A.J., Sinninghe Damsté, J.S., Hopmans, E.C., Schouten, S., 2010. Applicability and calibration of the TEX_{86} paleothermometer in lakes. *Organic Geochemistry* 41, 404–413.
- Prahl, F.G., Muehlhausen, L.A., Zahnle, D.L., 1988. Further evaluation of long-chain alkenones as indicators of paleoceanographic conditions. *Geochimica et Cosmochimica Acta* 52, 2303–2310.
- Prahl, F.G., Wakeham, S.G., 1987. Calibration of unsaturation patterns in long-chain ketone compositions for paleotemperature assessment. *Nature* 330, 367–369.
- Rosenthal, Y., Boyle, E.A., Labeyrie, L., 1997. Last glacial maximum paleochemistry and deepwater circulation in the Southern Ocean: evidence from foraminiferal cadmium. *Paleoceanography* 12, 787–796.
- Rueda, G., Rosell-Mele, A., Escala, M., Gyllencreutz, R., Backman, J., 2009. Comparison of instrumental and GDGT-based estimates of sea surface and air temperatures from the Skagerrak. *Organic Geochemistry* 40, 287–291.
- Schouten, S., Hopmans, E.C., Pancost, R.D., Sinninghe Damsté, J.S., 2000. Widespread occurrence of structurally diverse tetraether membrane lipids: evidence for the

- ubiquitous presence of low-temperature relatives of hyperthermophiles. *Proceedings of the National Academy of Sciences USA* 97, 14421–14426.
- Schouten, S., Hopmans, E.C., Schefuß, E., Sinninghe Damsté, J.S., 2002. Distributional variations in marine crenarchaeotal membrane lipids: a new tool for reconstructing ancient sea water temperatures? *Earth and Planetary Science Letters* 204, 265–274.
- Schouten, S., Forster, A., Panoto, F.E., Sinninghe Damsté, J.S., 2007. Towards calibration of the TEX₈₆ palaeothermometer for tropical sea surface temperatures in ancient greenhouse worlds. *Organic Geochemistry* 38, 1537–1546.
- Schouten, S., Eldrett, J., Greenwood, D.R., Harding, I., Baas, M., Sinninghe Damsté, J.S., 2008. Onset of long-term cooling of Greenland near the Eocene-Oligocene boundary as revealed by branched tetraether lipids. *Geology* 36, 147–150.
- Schouten, S., Hopmans, E.C., van der Meer, J., Mets, A., Bard, E., Bianchi, T., Diefendorf, A., Escala, M., Freeman, K., Furukawa, Y., Huguet, C., Ingalls, A., Menot-Combes, G., Nederbragt, A., Oba, M., Pearson, A., Pearson, E., Rosell-Mele, A., Schaeffer, P., Shah, S., Shanahan, T., Smith, R., Smittenberg, R., Talbot, H., Uchida, M., Van Mooy, B., Yamamoto, M., Zhang, Z., Sinninghe Damsté, J.S., 2009. An interlaboratory study of TEX₈₆ and BIT analysis using high performance liquid chromatography/mass spectrometry. *Geochemistry, Geophysics, Geosystems* 10, Q03012. <http://dx.doi.org/10.1029/2008GC002221>.
- Schouten, S., Hopmans, E.C., Sinninghe Damsté, J.S., 2013. The organic geochemistry of glycerol dialkyl glycerol tetraether lipids: a review. *Organic Geochemistry* 54, 19–61.
- Shackleton, N.J., 1967. Oxygen isotope analyses and Pleistocene temperatures reassessed. *Nature* 215, 15–17.
- Sinninghe Damsté, J.S., Ossebaar, J., Schouten, S., Verschuren, D., 2008. Altitudinal shifts in the distribution of branched tetraether lipids in soils from Mt. Kilimanjaro (Tanzania): implications for the MBT/CBT continental palaeothermometer. *Organic Geochemistry* 39, 1072–1076.
- Sinninghe Damsté, J.S., Ossebaar, J., Abbas, B., Schouten, S., Verschuren, D., 2009. Fluxes and distribution of tetraether lipids in an equatorial African lake: constraints on the application of the TEX₈₆ palaeothermometer and branched tetraether lipids in lacustrine settings. *Geochimica et Cosmochimica Acta* 73, 4232–4249.
- Sinninghe Damsté, J.S., Rijpstra, W.I.C., Hopmans, E.C., Weijers, J.W.H., Foesel, B.U., Overmann, J., Dedysh, S.N., 2011. 13,16-Dimethyl octacosanedioic acid (isodiaboloic acid), a common membrane-spanning lipid of *Acidobacteria* subdivisions 1 and 3. *Applied and Environmental Microbiology* 77, 4147–4154.
- Sinninghe Damsté, J.S., Rijpstra, W.I.C., Hopmans, E.C., Jung, M.-Y., Kim, J.-G., Rhee, S.-K., Stieglmeier, M., Schleper, C., 2012. Intact polar and core glycerol dibiphytanyl glycerol tetraether lipids of group I.1a and I.1b *Thaumarchaeota* in soil. *Applied and Environmental Microbiology* 78, 6866–6874.
- Sluijs, A., Schouten, S., Pagani, M., Woltering, M., Brinkhuis, H., Sinninghe Damsté, J.S., Dickens, G.R., Huber, M., Reichert, G.-J., Stein, R., Matthiessen, J., Lourens, L.J., Pedentchouk, N., Backman, J., Moran, K., the Expedition 302 Scientists, 2006. Subtropical Arctic ocean temperatures during the Palaeocene/Eocene thermal maximum. *Nature* 441, 610–613.
- Spang, A., Hatzepichler, R., Brochier-Armanet, C., Rattei, T., Tischler, P., Spieck, E., Streit, W., Stahl, D.A., Wagner, M., Schleper, C., 2010. Distinct gene set in two different lineages of ammonia-oxidizing archaea supports the phylum Thaumarchaeota. *Trends in Microbiology* 18, 331–340.
- Tierney, J.E., Russell, J.M., 2009. Distributions of branched GDGTs in a tropical lake system: implications for lacustrine application of the MBT/CBT paleoproxy. *Organic Geochemistry* 40, 1032–1036.
- Tierney, J.E., Russell, J.M., Eggermont, H., Hopmans, E.C., Verschuren, D., Sinninghe Damsté, J.S., 2010. Environmental controls on branched tetraether lipid distributions in tropical East African lake sediments. *Geochimica et Cosmochimica Acta* 74, 4902–4918.
- Timonen, S., Bomberg, M., 2009. Archaea in dry soil environments. *Phytochemistry Reviews* 8, 505–518.
- Wefer, G., Berger, W.H., 1991. Isotope paleontology: growth and composition of extant calcareous species. *Marine Geology* 100, 207–248.
- Weijers, J.W.H., Schouten, S., van der Linden, M., van Geel, B., Sinninghe Damsté, J.S., 2004. Water table related variations in the abundance of intact archaeal membrane lipids in a Swedish peat bog. *FEMS Microbiology Letters* 239, 51–56.
- Weijers, J.W.H., Schouten, S., Spaargaren, O.C., Sinninghe Damsté, J.S., 2006a. Occurrence and distribution of tetraether membrane lipids in soils: implications for the use of the TEX₈₆ proxy and the BIT index. *Organic Geochemistry* 37, 1680–1693.
- Weijers, J.W.H., Schouten, S., Hopmans, E.C., Geenevasen, J.A.J., David, O.R.P., Coleman, J.M., Pancost, R.D., Sinninghe Damsté, J.S., 2006b. Membrane lipids of mesophilic anaerobic bacteria thriving in peats have typical archaeal traits. *Environmental Microbiology* 8, 648–657.
- Weijers, J.W.H., Schefuß, E., Schouten, S., Sinninghe Damsté, J.S., 2007a. Coupled thermal and hydrological evolution of tropical Africa over the last deglaciation. *Science* 315, 1701–1704.
- Weijers, J.W.H., Schouten, S., Sluijs, A., Brinkhuis, H., Sinninghe Damsté, J.S., 2007b. Warm arctic continents during the Palaeocene-Eocene thermal maximum. *Earth and Planetary Science Letters* 261, 230–238.
- Weijers, J.W.H., Schouten, S., van den Donker, J.C., Hopmans, E.C., Sinninghe Damsté, J.S., 2007c. Environmental controls on bacterial tetraether membrane lipid distribution in soils. *Geochimica et Cosmochimica Acta* 71, 703–713.
- Weijers, J.W.H., Wiesenberg, G.L.B., Bol, R., Hopmans, E.C., Pancost, R.D., 2010. Carbon isotopic composition of branched tetraether membrane lipids in soils suggest a rapid turnover and a heterotrophic life style of their source organism(s). *Biogeosciences* 7, 2959–2973.
- West, A.E., Schmidt, S.K., 2002. Endogenous methanogenesis stimulates oxidation of atmospheric CH₄ in alpine tundra soil. *Microbial Ecology* 43, 408–415.
- Wuchter, C., Schouten, S., Coolen, M.J.L., Sinninghe Damsté, J.S., 2004. Temperature-dependent variation in the distribution of tetraether membrane lipids of marine Crenarchaeota: implications for TEX₈₆ paleothermometry. *Paleoceanography* 19, PA4028. <http://dx.doi.org/10.1029/2004PA001041>.
- Wuchter, C., Schouten, S., Wakeham, S.G., Sinninghe Damsté, J.S., 2005. Temporal and spatial variation in tetraether membrane lipids of marine Crenarchaeota in particulate organic matter: Implications for TEX₈₆ paleothermometry. *Paleoceanography* 20, PA3013. <http://dx.doi.org/10.1029/2004PA001110>.
- Xie, S., Pancost, R.D., Chen, L., Evershed, R.P., Yang, H., Zhang, K., Huang, J., Xu, Y., 2012. Microbial lipid records of highly alkaline deposits and enhanced aridity associated with significant uplift of the Tibetan Plateau in the Late Miocene. *Geology* 40, 291–294.
- Yang, H., Ding, W.H., Wang, J.X., Jing, C.S., He, G.Q., Qin, Y.M., Xie, S.C., 2012. Soil pH impact on microbial tetraether lipids and terrestrial input index (BIT) in China. *Science China Earth Sciences* 55, 236–245.
- Zhang, Y.G., Zhang, C.L., Liu, X.-L., Li, L., Hinrichs, K.-W., Noakes, J.E., 2011. Methane index: a tetraether archaeal lipid biomarker indicator for detecting the instability of marine gas hydrates. *Earth and Planetary Science Letters* 307, 525–534.